

# Steady-State and Dynamic Desorption of Organic Vapor from Activated Carbon with Electrothermal Swing Adsorption

HAMIDREZA EMAMIPOUR,<sup>†</sup>  
ZAHER HASHISHO,<sup>†</sup> DIEGO CEVALLOS,<sup>†</sup>  
MARK J. ROOD,<sup>\*,†,‡</sup>  
DEBORAH L. THURSTON,<sup>†,‡</sup>  
K. JAMES HAY,<sup>§</sup> BYUNG J. KIM,<sup>§</sup> AND  
PATRICK D. SULLIVAN<sup>||</sup>

Department of Civil and Environmental Engineering,  
University of Illinois at Urbana-Champaign, Urbana, Illinois  
61801, Industrial & Enterprise Systems Engineering, University  
of Illinois at Urbana-Champaign, Urbana, Illinois 61801,  
Engineer Research and Development Center, Construction  
Engineering Research Laboratory, Champaign, Illinois 61826,  
and Air Force Research Laboratory/MLQL, 139 Barnes Drive,  
Suite 2, Tyndall AFB, Florida 32403

A new method to achieve steady-state and dynamic-tracking desorption of organic compounds from activated carbon was developed and tested with a bench-scale system. Activated carbon fiber cloth (ACFC) was used to adsorb methyl ethyl ketone (MEK) from air streams. Direct electrothermal heating was then used to desorb the vapor to generate select vapor concentrations at 500 ppmv and 5000 ppmv in air. Dynamic-tracking desorption was also achieved with carefully controlled yet variable vapor concentrations between 250 ppmv and 5000 ppmv, while also allowing the flow rate of the carrier gas to change by 100%. These results were also compared to conditions when recovering MEK as a liquid, and using microwaves as the source of energy to regenerate the adsorbent to provide MEK as a vapor or a liquid.

## Introduction

There are numerous industrial processes (e.g., coating operations) that generate organic vapors with a wide range of highly variable concentrations (e.g., paint spray booths). Many of these gas streams need to be treated by devices such as biofilters or oxidizers before the gas streams are emitted to the atmosphere. Such variable vapor concentrations make it challenging to effectively remove the vapors from the gas streams without over-sizing the biofilter or oxidizer to achieve a specified removal efficiency of the vapor, or to produce more than necessary CO<sub>2</sub> emissions from burning excessive amounts of auxiliary fuel with a thermal oxidizer (1–6). Combining adsorption with concentration-controlled

\* Corresponding author phone: (217) 333-6963; fax: (217) 333-6968; e-mail: mrood@uiuc.edu.

† Department of Civil and Environmental Engineering, University of Illinois at Urbana-Champaign.

‡ Industrial and Enterprise Systems Engineering, University of Illinois at Urbana-Champaign.

§ Engineer Research and Development Center, Construction Engineering Research Laboratory.

|| Air Force Research Laboratory/MLQL.

desorption to an pretreat gas streams upstream of a biofilter or an oxidizer was reviewed for a wide range of systems and was then discussed in detail for a microwave swing adsorption (MSA) system (7). The MSA system used activated carbon fiber cloth (ACFC) adsorbent to remove methyl ethyl ketone (MEK) from air streams and then steady-state tracking desorption to provide a readily controllable feed stream of that vapor in air at a specified concentration and a constant gas flow rate.

In this research, a bench-scale electrothermal swing adsorption (ESA) system (8) that was developed to capture a wide range of organic vapors from gas streams and recover them as a liquid stream with in-vessel condensation was modified to allow for adsorption and then steady-state tracking (SST) desorption of that vapor. The system was modified to control its outlet vapor concentration during desorption cycles based on user-defined constant or dynamic set-points that were independent of gas flow rate or inlet concentration for the conditions that were tested. This well-defined concentration of organic vapor could then be treated at low concentrations (100s ppmv) with biofiltration or at high concentrations (1000s ppmv) by oxidation at a specified gas flow rate (Figure 1).

## Experimental Section

**Experimental Setup.** The bench-scale system used to evaluate the performance of ESA-SST desorption consisted of a vapor generation system, adsorption/regeneration vessel, organic vapor detector, and a data acquisition/instrumentation control system (Figure 2). The vapor generator consisted of a source of filtered compressed air, a custom silica gel adsorber, a mass flow controller (Aalborg, model GFC571S), and a syringe pump (KD Scientific, model 200) with a 100 mL syringe (Hamilton). The adsorption/regeneration vessel consisted of an aluminum cylinder and conical base with a Teflon top plate. The external diameter of the vessel was 15.2 cm with a wall thickness of 1.9 cm. The cylindrical and conical portions of the vessel were 23.5 and 8.2 cm tall, respectively (8). The top plate was made of Teflon to ensure electrical isolation of the ACFC during electrothermal regeneration of the ACFC. Two annular cartridges of ACFC (American Kynol, ACC-5092-20) with a total weight of 73.5 g were located vertically in the cylindrical portion of the vessel. The external diameter of the cartridges was 3.1 cm with a length of 20 cm. Temperatures of the cartridges and external wall of the vessel were measured with Type K thermocouples (0.0254 cm diameter, Omega Inc.) that were located at the vertical center of the cartridges and the cylindrical portion of the vessel's external wall. Cartridge temperature is reported as the mean value for the two cartridges. During the adsorption cycle, the gas stream entered the bottom of the vessel's cylindrical section, passed through the cartridges in parallel from the outside to the inside of the cartridges, and then exited through the top of the vessel. The organic vapor concentration was detected at the vessel's outlet with a photoionization detector (PID, RAE Systems Inc., PDM-10A). Regeneration of the ACFC occurred by direct electrothermal heating of the adsorbent while air passed from the top of the vessel, through both cartridges from their inside to their outside, and then exited through the bottom of the vessel. The measured electrical power applied to the cartridges ( $Q_{e,m}$ ) was determined with root mean squared voltage and current values obtained from the fully automatic microprocessor-based measurement and control system (National Instruments Inc.) using Labview software. There was no operator

<b>Report Documentation Page</b>			Form Approved OMB No. 0704-0188		
<p>Public reporting burden for the collection of information is estimated to average 1 hour per response, including the time for reviewing instructions, searching existing data sources, gathering and maintaining the data needed, and completing and reviewing the collection of information. Send comments regarding this burden estimate or any other aspect of this collection of information, including suggestions for reducing this burden, to Washington Headquarters Services, Directorate for Information Operations and Reports, 1215 Jefferson Davis Highway, Suite 1204, Arlington VA 22202-4302. Respondents should be aware that notwithstanding any other provision of law, no person shall be subject to a penalty for failing to comply with a collection of information if it does not display a currently valid OMB control number.</p>					
1. REPORT DATE <b>2007</b>	2. REPORT TYPE	3. DATES COVERED <b>00-00-2007 to 00-00-2007</b>			
<b>4. TITLE AND SUBTITLE</b> <b>Steady-State and Dynamic Desorption of Organic Vapor From Activated Carbon With Electrothermal Swing Adsorption</b>			5a. CONTRACT NUMBER		
			5b. GRANT NUMBER		
			5c. PROGRAM ELEMENT NUMBER		
<b>6. AUTHOR(S)</b>			5d. PROJECT NUMBER		
			5e. TASK NUMBER		
			5f. WORK UNIT NUMBER		
<b>7. PERFORMING ORGANIZATION NAME(S) AND ADDRESS(ES)</b> <b>Department of Civil and Environmental Engineering, University of Illinois at Urbana-Champaign, Urbana, IL, 61801</b>			8. PERFORMING ORGANIZATION REPORT NUMBER		
<b>9. SPONSORING/MONITORING AGENCY NAME(S) AND ADDRESS(ES)</b>			10. SPONSOR/MONITOR'S ACRONYM(S)		
			11. SPONSOR/MONITOR'S REPORT NUMBER(S)		
<b>12. DISTRIBUTION/AVAILABILITY STATEMENT</b> <b>Approved for public release; distribution unlimited</b>					
<b>13. SUPPLEMENTARY NOTES</b> <b>U.S. Government or Federal Rights.</b>					
<b>14. ABSTRACT</b>					
<b>15. SUBJECT TERMS</b>					
<b>16. SECURITY CLASSIFICATION OF:</b> a. REPORT      b. ABSTRACT      c. THIS PAGE <b>unclassified</b> <b>unclassified</b> <b>unclassified</b>			<b>17. LIMITATION OF ABSTRACT</b> <b>Same as Report (SAR)</b>	<b>18. NUMBER OF PAGES</b> <b>7</b>	<b>19a. NAME OF RESPONSIBLE PERSON</b>

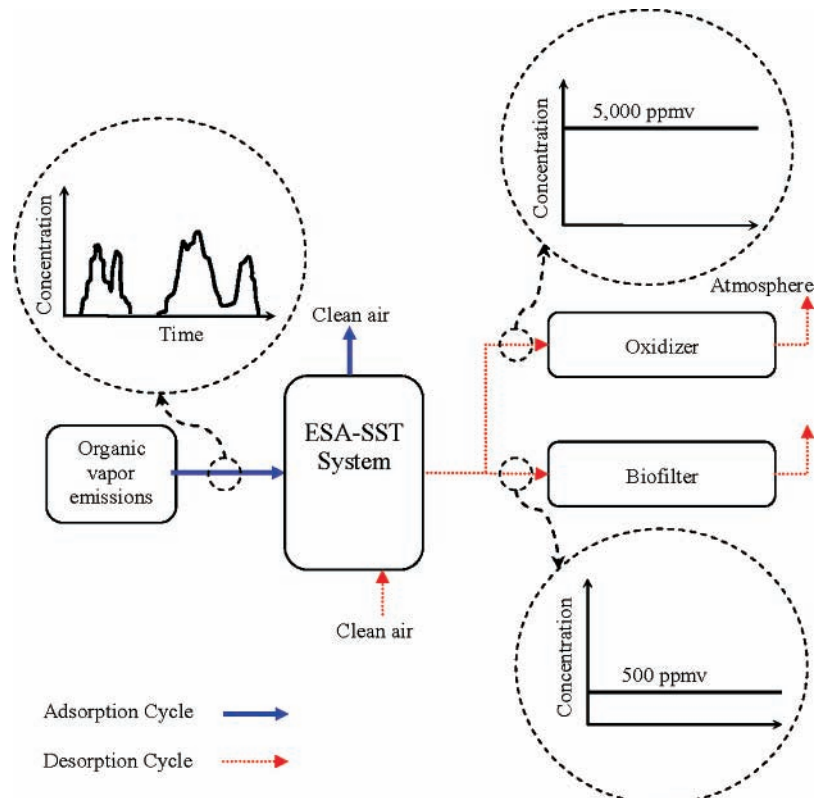


**FIGURE 1.** ESA-SST pretreatment system upstream of a biofilter or oxidizer.

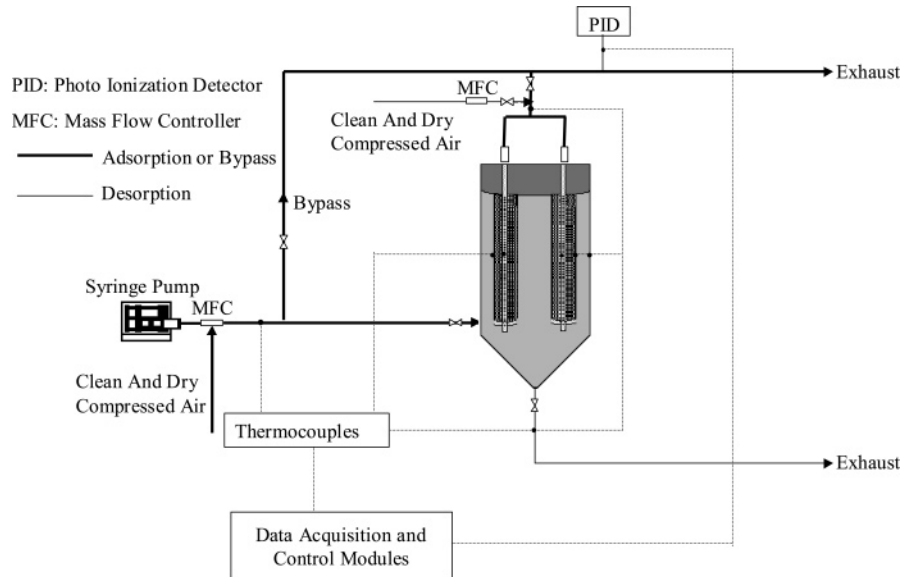


**FIGURE 2.** Bench-scale ESA-SST system.

intervention of the data acquisition and control system during the adsorption or regeneration tests.

**Methodology.** The syringe pump injected liquid MEK (HPLC grade, >99% purity, Sigma Aldrich) into the dry and clean air stream to generate the vapor-laden gas stream that contained the specified concentration of MEK. A material balance for the MEK and air streams was used to calibrate the PID with multi-point calibrations at the gas flow rates used to complete the ESA-SST tests. The outlet gas stream was diluted with dry/clean air during the desorption cycles at high concentration (5000 ppmv) and the dynamic tracking test to prevent saturation of the PID sensor.

All adsorption tests were performed at an inlet air flow rate of 100 slpm (standard liters per minute, at standard

temperature and pressure, STP = 0 °C, 101 kPa) and 500 ppmv of MEK. Nominal laboratory conditions were 25 °C and 98 kPa. The gas stream initially bypassed the vessel before each adsorption test, until the MEK concentration in the air stream achieved its specified steady-state value. The adsorption cycle then occurred with the MEK-laden gas stream passing through the vessel until the vessel's adsorbent was >98% saturated with MEK. The total amount of MEK adsorbed at saturation was estimated by multiplying the amount of time to achieve 50% breakthrough curve by the mass feed rate of MEK vapor flowing into the system.

SST desorption tests were performed at an air flow rate of 20 slpm for the 500 ppmv MEK test and 10 slpm for the 5000 ppmv MEK test. The dynamic-tracking desorption test

**TABLE 1. Parameters Used for the ESA-SST System's Energy Balance**

parameter	description	value	unit
$m_{\text{ACFC}}$	total mass of adsorbent cartridges	73.53	g
$c_{p,\text{ACFC}}$	heat capacity of adsorbent <sup>a</sup>	0.971 (11)	J g <sup>-1</sup> K <sup>-1</sup>
$m_{\text{MEK}}$	mass of MEK remaining in the adsorbent	f(t)	g
$c_{p,\text{MEK}}$	heat capacity of liquid MEK	2.19 (9)	J g <sup>-1</sup> K <sup>-1</sup>
$m_{\text{fittings}}$	total mass of the fittings	366	g
$c_{p,\text{fittings}}$	heat capacity of the fittings	0.47 (11)	J g <sup>-1</sup> K <sup>-1</sup>
$T$	temperature of the cartridges	f(t) <sup>b</sup>	K
$t$	time	-	s
$M_{\text{air}}$	molecular weight of air	28.97	g-mol <sup>-1</sup>
$T_{\text{in}}$	temperature of air at the inlet of the vessel	298	K
$c_{p,\text{air}}$	heat capacity of air	f(T)	J g <sup>-1</sup> K <sup>-1</sup>
$h_c$	convective heat transfer coefficient	f(T) (9)	W m <sup>-2</sup> K <sup>-1</sup>
$A_c$	external surface area of cartridges	0.039	m <sup>2</sup>
$T_w$	temperature of vessel wall	f(t)	K
$\sigma$	Stefan-Boltzmann constant	5.667 × 10 <sup>-8</sup>	W m <sup>-2</sup> K <sup>-4</sup>
$\epsilon_{\text{ACFC}}$	emissivity of ACFC	0.9 (9)	-
$\epsilon_w$	emissivity of vessel wall	0.09 (10)	-
$F_{c-w}$	radiation shape factor	0.922	-
$A_w$	internal area of the vessel wall	0.0982	m <sup>2</sup>
$\Delta H_{\text{ads}}$	isosteric heat of adsorption	700 (18)	J g <sup>-1</sup>
$\dot{m}_{\text{MEK}}$	mass flow rate of desorbed MEK	f(t)	g s <sup>-1</sup>

<sup>a</sup> Same as graphite. <sup>b</sup> Varies with time.

occurred with variable pre-defined set-points ranging from 250 to 5000 ppmv, and 10 or 20 slpm. The concentration of MEK at the vessel's outlet during the regeneration tests was controlled with the use of proportional-integral-derivative control of the electrical power applied to the ACFC to achieve the desired set-point concentrations. Repetitive adsorption and regeneration tests were performed to make sure the results were reproducible and consistent. No deterioration in the performance of the ACFC was noticed after 11 adsorption and steady-state regeneration tests. Performance criteria included breakthrough times, amounts of vapor adsorbed at breakthrough, and the temperature achieved by the ACFC at select power settings.

The total mass of MEK that desorbed during each desorption cycle ( $m_d$ ) was calculated using a material balance for the MEK

$$m_d = \frac{\dot{V}_{\text{air}} P^0 M_{\text{MEK}}}{RT^0} \sum_{t=0}^{t_{\text{reg}}} \frac{y_{\text{out}}}{1 - y_{\text{out}}} \delta t \quad (1)$$

where  $\dot{V}_{\text{air}}$  = flow rate of air during the regeneration cycle at STP;  $P^0$  = standard pressure;  $M_{\text{MEK}}$  = molecular weight of MEK;  $R$  = ideal gas law constant;  $T^0$  = standard temperature,  $t_{\text{reg}}$  = total regeneration time;  $y_{\text{out}}$  = mole fraction of MEK in the outlet gas stream; and  $\delta t$  = time interval. The extent of adsorbent regeneration ( $\eta_{\text{reg}}$ ) is defined as the percent of the initially adsorbed MEK that was desorbed during the regeneration cycle

$$\eta_{\text{reg}} = \frac{m_d}{m_{\text{ai}}} \times 100 \quad (2)$$

where  $m_{\text{ai}}$  = amount of initially adsorbed MEK during the preceding adsorption cycle. The extent of adsorbent regeneration was also characterized by assuming equilibrium conditions,  $\eta_{\text{reg},\text{eq}}$ , and is defined as the percent of the adsorbed MEK that is desorbed during the regeneration cycle assuming the MEK in the gas stream is in equilibrium with adsorbed MEK

$$\eta_{\text{reg},\text{eq}} = \frac{m_{\text{ai},\text{eq}} - m_{\text{a},\text{eq}}}{m_{\text{ai},\text{eq}}} \times 100 \quad (3)$$

where  $m_{\text{ai},\text{eq}}$  is the initial equilibrium loading of MEK from

the previous adsorption cycle, and  $m_{\text{a},\text{eq}}$  is the equilibrium loading of MEK that was calculated based on the MEK concentrations in the bulk gas stream, temperature of the cartridge, and the Dubinin–Radushkevich (DR) isotherm equation (12).

An energy balance for the control volume around both of the ACFC cartridges and fittings was developed based on Sullivan et al.'s work (9) to calculate the energy applied to the cartridges ( $\dot{Q}_{\text{e,c}}$ ) during the regeneration cycles (eq 4). The energy balance considered the (1) specific heats of the adsorbent, adsorbed MEK, cartridges' fittings, and air; (2) convective heat transfer; (3) radiative heat transfer; and (4) isosteric heat of adsorption of MEK (Table 1).

$$\begin{aligned} \dot{Q}_{\text{e,c}} = & (m_{\text{ACFC}} c_{p,\text{ACFC}} + m_{\text{MEK}} c_{p,\text{MEK}} + m_{\text{fittings}} c_{p,\text{fittings}}) \frac{dT}{dt} + \\ & \frac{\dot{V}_{\text{air}} P^0 M_{\text{Air}}}{RT^0} \int_{T_{\text{in}}}^T c_{p,\text{air}} dT + h_c A_c (T - T_w) + \\ & \frac{\sigma (T^4 - T_w^4)}{(1 - \epsilon_{\text{ACFC}}) + \frac{1}{A_c F_{c-w}} + \frac{(1 - \epsilon_w)}{\epsilon_w A_w}} + \Delta H_{\text{ads}} m_{\text{MEK}} \quad (4) \end{aligned}$$

The heat transfer coefficient,  $h_c$ , was calculated by the same correlation that was used by Sullivan et al. (9). The general method to calculate the radiation shape factor,  $F_{c-w}$ , was provided by Mills (11). The temperature of the cartridges' fittings and the cartridges were assumed to be the same.

The absolute relative difference (ARD) is used to compare the difference between two relevant properties and is defined by:

$$\text{ARD} = \frac{1}{N} \sum_{i=1}^N \left[ \frac{|x_i^{(1)} - x_i^{(2)}|}{x_i^{(1)}} \times 100 \right] \quad (5)$$

where  $N$  is the total number of corresponding data points, and  $x^{(1)}$  and  $x^{(2)}$  represent corresponding properties of interest.

## Results and Discussion

The MEK concentration at the outlet of the vessel and the corresponding set-point of 500 ppmv, the temperature of the cartridges and vessel,  $\eta_{\text{reg}}$  and  $\eta_{\text{reg},\text{eq}}$ , and  $\dot{Q}_{\text{e,m}}$  and cumulative energy during SST desorption are described in

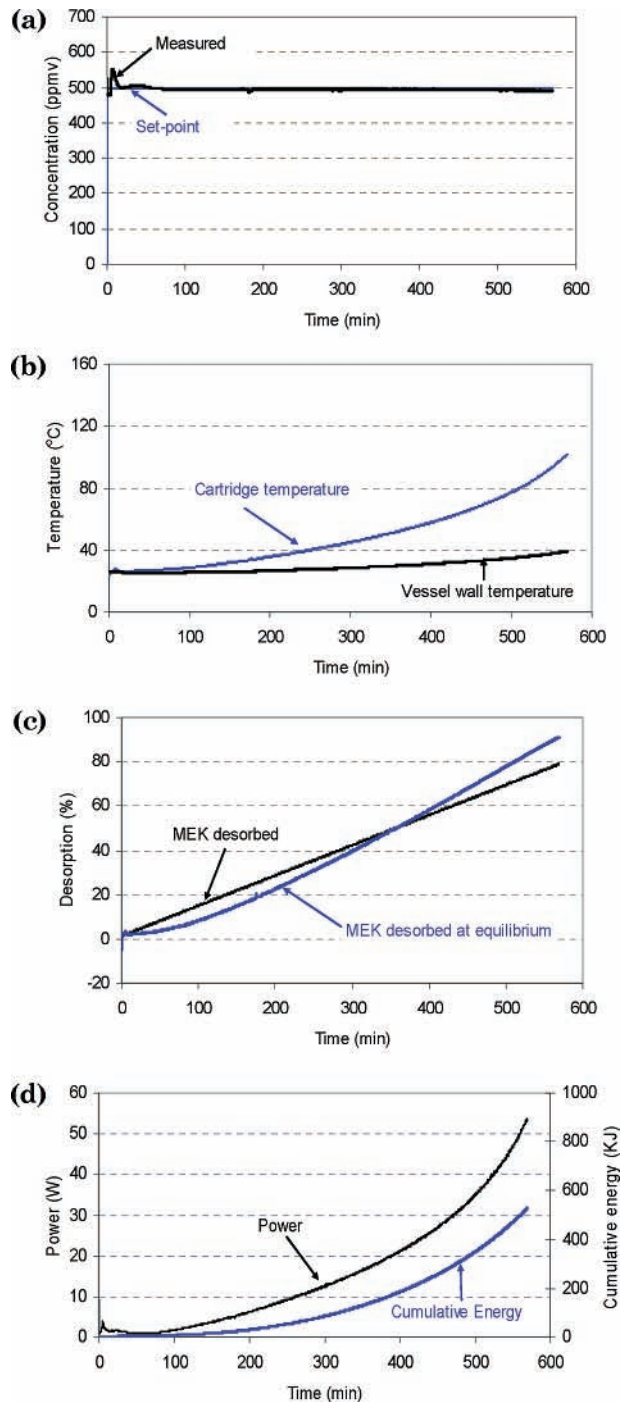


**FIGURE 3.** Steady-state tracking desorption test results to achieve a MEK concentration of 500 ppmv in 20 slpm air: (a) the vessel's outlet vapor concentration with a set-point of 500 ppmv; (b) temperature of the ACFC and the vessel wall; (c) extent of regeneration of the ACFC; and (d) power and cumulative energy deposited to the ACFC.

Figures 3a–d, respectively. The measured MEK outlet concentration was  $496 \pm 3$  ppmv (average  $\pm$  standard deviation). The ARD between the set-point and the measured MEK concentration was 0.94%. Temperature of the adsorbent increased from 25 to 100 °C because of the additional energy applied to the cartridges to maintain the constant outlet concentration despite the reduction in the amount of adsorbed MEK as time elapsed during the test. The ARD of 20% between  $\eta_{\text{reg}}$  and  $\eta_{\text{reg},\text{eq}}$  is most likely due to the assumption of equilibrium between vapor phase and adsorbed phase, possible heterogeneity within the adsorbent,

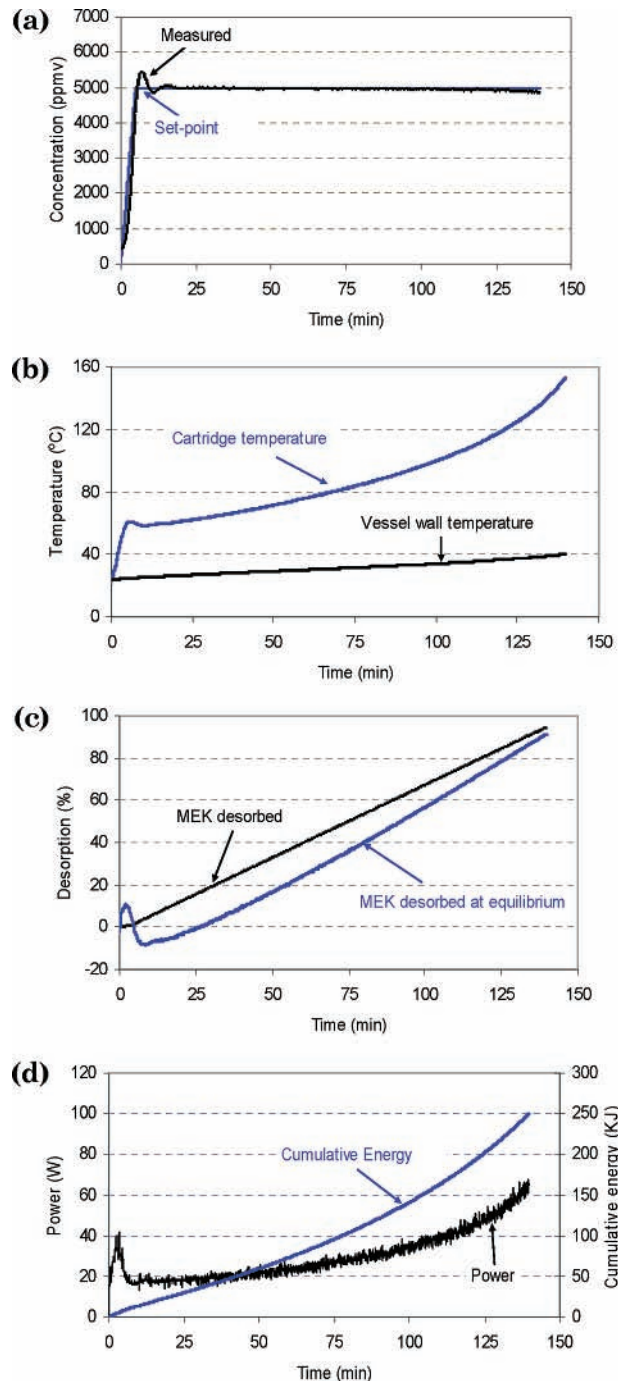


**FIGURE 4.** Steady-state tracking desorption test results to achieve an MEK outlet concentration of 5000 ppmv at 10 slpm in air: (a) the vessel's outlet vapor concentration with a set-point of 5000 ppmv; (b) temperature of the ACFC and the vessel wall; (c) extent of regeneration of the ACFC; and (d) power and cumulative energy deposited to the ACFC.

and use of the DR equation (Figure 3c). Assuming equilibrium, conditions should be reasonable due to the ACFC's small fiber diameter of  $12.3 \pm 1 \mu\text{m}$  (13). However, adsorbate loading and temperature may not be uniformly distributed in the cartridges. Also, the DR equation has an ARD  $\leq 9.2\%$  when comparing measured and modeled equilibrium adsorption capacities for the ACFC-MEK system between 20 and 175 °C (12). The average  $\dot{Q}_{e,\text{m}}$  value was 15.5 W resulting in an energy per unit mass of desorbed MEK of 28.6 kJ/g.

Desorption of MEK at a constant set-point of 5000 ppmv resulted in a measured MEK outlet concentration of  $4962 \pm 32$  ppmv and an ARD of 0.8% between these two parameters

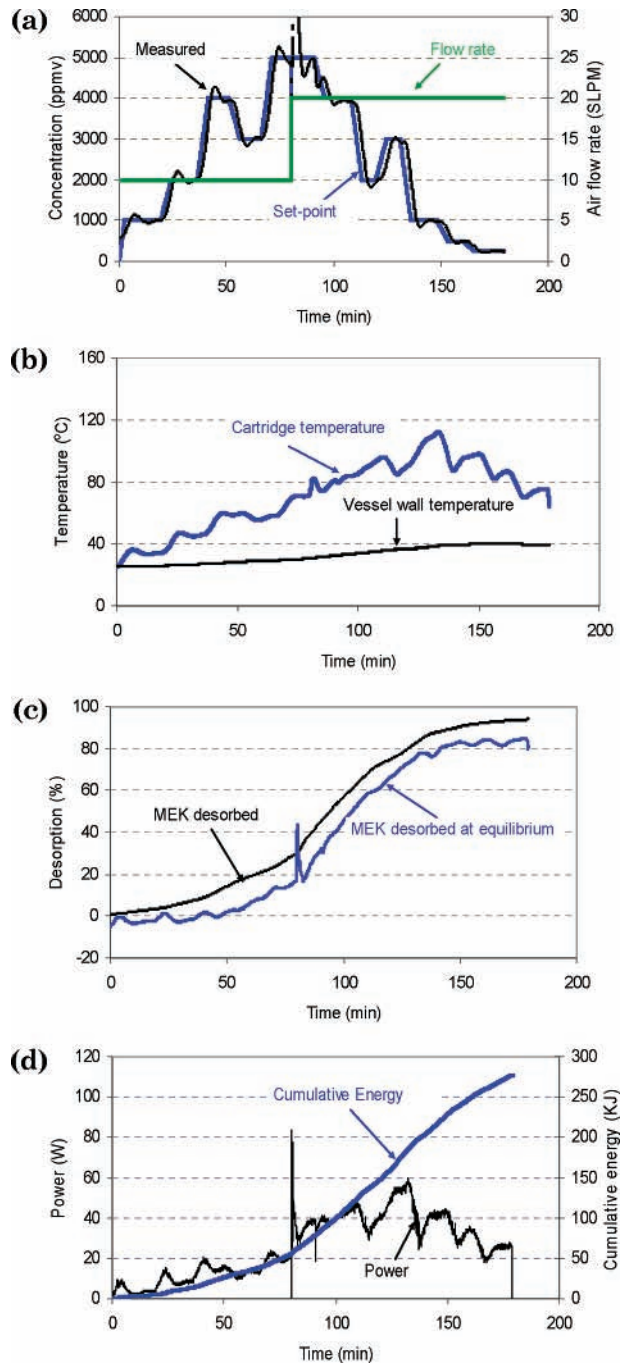


**FIGURE 5.** Dynamic tracking desorption test results to achieve MEK outlet concentrations between 250 ppmv and 5000 ppmv at 10 and 20 slpm in air: (a) the vessel's outlet vapor concentration with a variable set-point; (b) temperature of the ACFC and the vessel wall; (c) extent of regeneration of the ACFC; and (d) power and cumulative energy deposited to the ACFC.

(Figure 4). Maximum temperature of the adsorbent was 152 °C, which is 52 °C more than the test at 500 ppmv MEK because more power was required to achieve a faster rate of desorption to obtain the higher set-point concentration. The average  $\dot{Q}_{e,m}$  value was 25.8 W resulting in an energy per unit mass of desorbed MEK of 9.9 kJ/g. Although more power is required at a higher outlet concentration, the duration of the desorption cycle is less, and the electrical energy is 65% less than for the 500 ppmv case. Discussion about the distribution of energy during each desorption cycle is described later.

Results from the dynamic SST outlet concentration tests at two air flow rates demonstrate that the system is very

**TABLE 2. Energy Consumed for MEK Recovered as Liquid and Vapor**

desorption technique	energy/mass of adsorbate produced as liquid (R) or as vapor (SST) (kJ/g)
ESA-R	2.5–24.5 (8)
ESA-SST	9.9–28.6
MSA-R	6.6–19.8 (16)
MSA-SST	16.1–38.7 (7)

responsive at controlling the concentration of MEK based on the set-points with an ARD between the measured and set-point concentrations of 2.8% (Figure 5a). The sharp spikes in the middle of the plots in Figure 5 are due to the specified air flow rate increasing by 100% and the change in the dilution ratio for the PID. However, the controller quickly responded to return the outlet MEK concentration to its set-point value. The temperature of the cartridges ranged between 25 and 112 °C as  $\dot{Q}_{e,m}$  increased or decreased between 1.0 and 84 W. The average  $\dot{Q}_{e,m}$  was 22 W resulting in an energy per unit mass of desorbed MEK of 9.2 kJ/g.

The concentration of MEK at the outlet of the vessel was kept below its lower flammable limit (LFL) in air during all desorption tests. It is important to keep the concentration of flammable vapors below their LFL if regeneration occurs with sufficient oxygen to sustain a flame. LFL for MEK in air is calculated by (14)

$$LFL_T = LFL_{25^\circ C} \left[ 1 - \frac{0.75(T - 25)}{\Delta H_C} \right] \quad (6)$$

where  $T$  is the temperature of the air (°C),  $\Delta H_C$  is the net heat of combustion (kcal/mol), and the subscripts define the temperature for the LFL of MEK vapor in air. The maximum temperature during all of the desorption tests was 156 °C. The LFL at this temperature is 14 773 ppmv, which is 200% higher than the maximum MEK set-point concentration of 5000 ppmv. It should be noted that MEK concentration is higher within the ACFC's pores than the bulk gas, but the maximum temperature experienced by the adsorbent was less than the autoignition temperature of 514 °C for the bulk MEK concentration in air, and no fires were observed during the regeneration tests.

The electrothermal/microwave swing adsorption-recovery systems (ESA-R/MSA-R) remove organic vapors from gas streams with ACFC and recover the vapors as liquids with electrothermal/microwave regeneration of the ACFC with rapid in-vessel condensation of the organic vapors (8, 9, 15, 16). This approach promotes recovery of the organic vapors as a liquid and helps to provide a more sustainable technology. However, when recovery with the MSA-R/ESA-R systems is not feasible, then destroying these pollutants can be more applicable.

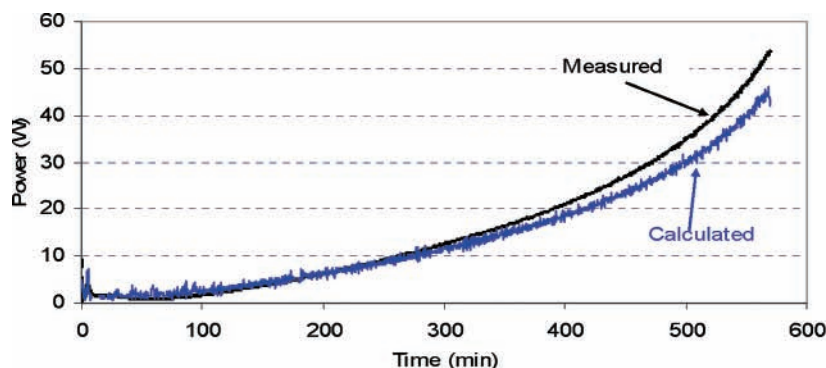
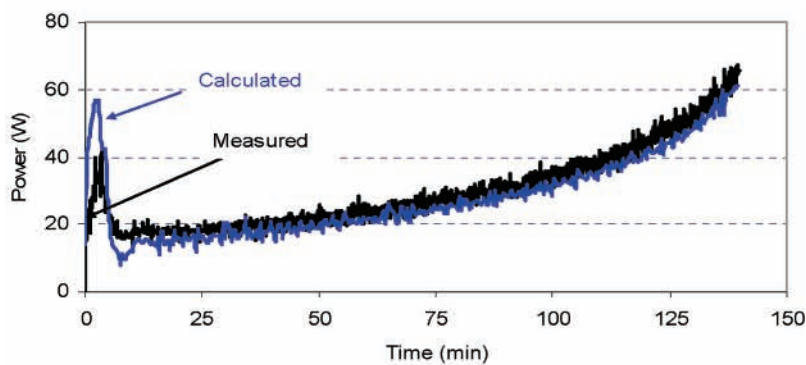
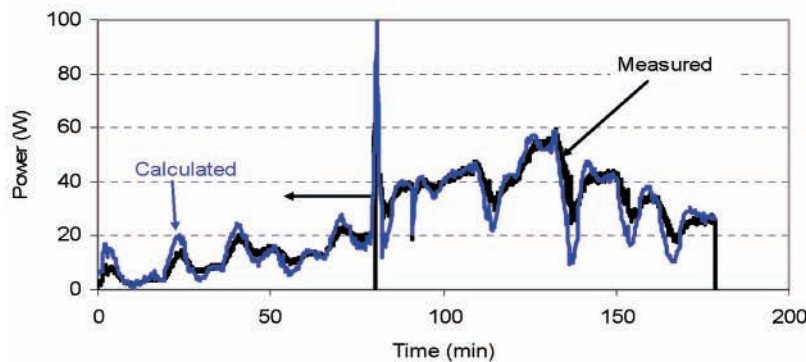
The net energy consumed while regenerating ACFC when using ESA-R, ESA-SST, MSA-R, and MSA-SST are described in Table 2. These values are based on all the bench-scale experimental tests. Energy applied to the ACFC for the liquid recovery tests and the steady-state vapor generation tests ranges from 2.5 to 24.5 kJ/g of MEK and 9.9 to 38.7 kJ/g of MEK, respectively. These values do not provide sufficient justification to favor one or the other method. However, liquid recovery (ESA-R and MSA-R) of flammable vapors should not occur in air because the vapor concentrations in the bulk gas can exist between the upper and lower flammability limits for the vapor. Therefore an inert gas such as N<sub>2</sub> is used

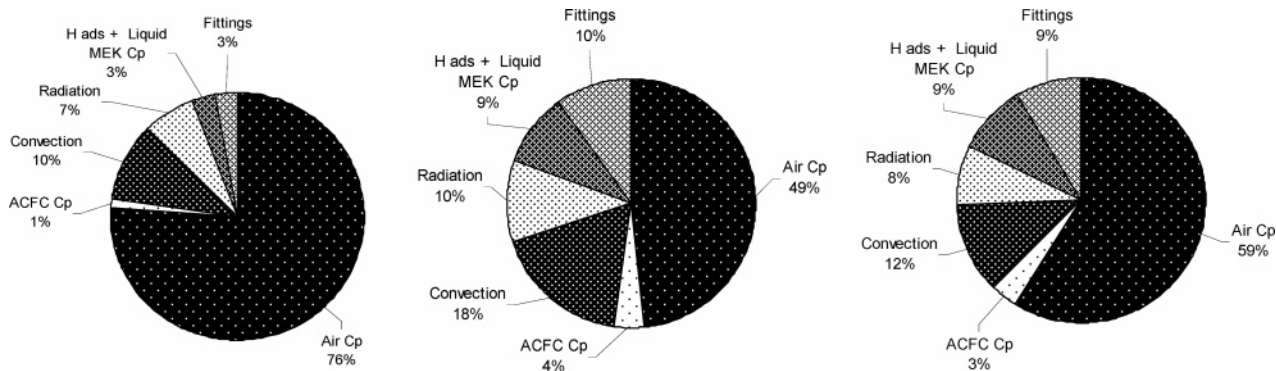
**TABLE 3. Advantages and Disadvantages of ESA and MSA Systems**

system	advantages	disadvantages
ESA	simple to design and operate more cost-effective can readily use different shapes of ACFC (e.g., pleated filter, cylinder)	possibility of electrical channeling depending on the type of adsorbent and its configuration not possible to achieve selective desorption based on the system's microwave properties
MSA	potential for selective desorption based on microwave properties can use different types of adsorbents (e.g., granular, fiber, felt, cloth) can readily use different shape of ACFC (e.g., pleated filter, cylinder)	more complicated to transform microwave energy to thermal energy higher cost for power supply

to displace O<sub>2</sub> from the vessel and as a carrier gas during the regeneration cycles. The amount of energy required by an air compressor to generate N<sub>2</sub> from ambient air with a membrane-based gas separation device was 3.3 times the

total energy required to regenerate ACFC (18) for a pilot-scale ESA-R system. Consequently, recovery of MEK as a liquid requires 10% to 270% more energy to regenerate the adsorbent than for steady-state desorption. These values are

**A- Steady-state desorption with a set-point of 500 ppmv****B- Steady-state desorption with a set-point of 5,000 ppmv****C- Dynamic tracking the specified outlet vapor concentration of 250 ppmv to 5,000 ppmv****FIGURE 6. Calculated and measured electrical power for the three desorption scenarios.**



**A- Steady state tracking desorption with a set-point of 500 ppmv**

**B- Steady state tracking desorption with a set-point of 5,000 ppmv**

**C- Dynamic tracking desorption with set-points from 250 ppmv to 5,000 ppmv**

**FIGURE 7. Energy distribution for steady state and dynamic tracking desorption tests.**

considerably larger than the isosteric heat of adsorption for the MEK-ACFC system of 0.7 kJ/g (18).

The amounts of energy consumed for the ESA and MSA systems are of the same order of magnitude. However, depending on the type of application one system might be favorable over the other (Table 3). For instance, the MSA has the potential for selective desorption based on the microwave properties of the adsorbent and adsorbate which can enhance the energy efficiency of the system. In contrast, the ESA system is less complex than the MSA system and allows for direct application of energy to the adsorbent.

Comparison of  $\dot{Q}_{e,m}$  to  $\dot{Q}_{e,c}$  resulted in ARD values <30% between those parameters for all three types of regeneration tests (Figure 6). The distributions of deposited energy once 80% of the MEK was desorbed from the ACFC (Figures 3–5) were determined with integration of eq 4 (Figure 7). Sensible heat for the gas is the largest energy term (49–76%), as it increased with decreasing temperature and decreasing MEK outlet concentration, but increased with increasing duration of the desorption cycle. Convection energy was the distant second largest term (10–18%), as it increased with increasing temperature and increasing MEK concentration, but decreased with increasing duration of the desorption cycle.

These results demonstrate that steady-state and dynamic-tracking desorption of organic vapor can be readily achieved with ESA technology to provide a gas stream with a readily controlled gas flow rate and organic vapor concentration, even if there is a rapid change in total gas flow rate. The resulting gas stream could be tailored for further processing in a manufacturing process, or treated at a high concentration by an oxidizer or at a low concentration by a biofilter.

### Acknowledgments

Financial support is acknowledged from the Department of Defense under contracts W9132T-04-2-0006 and A5639 FA8651-04-1-0004, and from the National Science Foundation grants DMI-02-17491 and BES-05-04385.

### Literature Cited

- (1) Cox, H. H. J.; Deshusses, M. A. Effect of starvation on the performance and re-acclimation of biotrickling filters for air pollution control. *Environ. Sci. Technol.* **2002**, *36*, 3069–3073.
- (2) Kim, D.; Cai, Z. G.; Sorial, G. A. Behavior of trickle-bed air biofilter for toluene removal: Effect of non-use periods. *Environ. Prog.* **2005**, *24*, 155–161.
- (3) Martin, F. J.; Loehr, R. C. Effect of periods of non-use on biofilter performance. *J. Air Waste Manage. Assoc.* **1996**, *46*, 539–546.
- (4) Moe, W. M.; Qi, B. Performance of a fungal biofilter treating gas-phase solvent mixtures during intermittent loading. *Water Res.* **2004**, *38*, 2259–2268.
- (5) Li, C. N.; Moe, W. M. Activated carbon load equalization of discontinuously generated acetone and toluene mixtures treated by biofiltration. *Environ. Sci. Technol.* **2005**, *39*, 2349–2356.
- (6) Morrone, P.; Di Maio, F. P.; Di Renzo, A.; Amelio, M. Modeling process characteristics and performance of fixed and fluidized bed regenerative thermal oxidizer. *Ind. Eng. Chem. Res.* **2006**, *45*, 4782–4790.
- (7) Hashisho, Z.; Emamipour, H.; Cevallos, D.; Rood, M.; Hay, K. J.; Kim, B. J. Rapid response concentration-controlled desorption of activated carbon to dampen concentration fluctuations. *Environ. Sci. Technol.* **2007**, *41*, 1753–1758.
- (8) Emamipour, H.; Kaldare, A.; Rood, M. J.; Thurston, D. Experimental study of cyclic adsorption/desorption of MEK in an ESA device. Presented at the 98th Annual Meeting of the Air & Waste Management Association, Minneapolis, MN, 2005; paper no. 1282, p 11.
- (9) Sullivan, P. D.; Rood, M. J.; Grevillot, G.; Wander, J. D.; Hay, K. J. Activated carbon fiber cloth electrothermal swing adsorption system. *Environ. Sci. Technol.* **2004**, *38*, 4865–4877.
- (10) Holman, J. P. *Heat Transfer*, 5th ed.; McGraw-Hill: New York, 1981.
- (11) Mills, A. F. *Heat Transfer*, 2nd ed.; Prentice Hall: Upper Saddle River, NJ, 1999.
- (12) Ramirez, D.; Sullivan, P. D.; Rood, M. J.; Hay, K. J. Equilibrium adsorption of phenol-, tire- and coal-derived activated carbons for organic vapors. *J. Environ. Eng.* **2004**, *130*, 231–241.
- (13) Lo, S. Characterization of the chemical, physical, thermal, and electrical properties of a series of activated carbon fiber cloths; Masters Thesis, University of Illinois at Urbana-Champaign, 2003; pp 86–88.
- (14) Crowl, D. A.; Louvar, J. F. *Chemical Process Safety: Fundamentals with Applications*, 2nd ed.; Prentice Hall PTR: Upper Saddle River, NJ, 2002.
- (15) Ramirez, D.; Vidal, E. X.; Rood, M. J. *Capture and recovery of vapor emissions from a painting facility in Fort Hood with an electrothermal–swing adsorption system*; second field campaign report; Engineer Research and Development Center–Construction Engineering Research Laboratory: Champaign, IL, 2004.
- (16) Hashisho, Z.; Rood, M.; Botich, L. Fixed-Bed Microwave-Swing Adsorption System to Capture and Recover Organic Vapors from Air Streams. *Environ. Sci. Technol.* **2005**, *39* (17), 6851.
- (17) Ramirez, D.; Lehmann, C. M. B.; Rood, M. J.; Hay, K. J. Adsorption of organic vapors on tire-, coal and phenol-derived activated carbons. Presented at the 94th Annual Meeting of the Air & Waste Management Association, Orlando, FL, 2001; paper no. 456, p 20.
- (18) Ramirez, D. Capture and recovery of organic vapors with an electrothermal swing adsorption system, Ph.D. Thesis, University of Illinois at Urbana-Champaign, 2005; p 120.

Received for review February 6, 2007. Revised manuscript received April 25, 2007. Accepted May 3, 2007.

ES0703022